Soft Matter

Accepted Manuscript

ROYAL SOCIETY OF CHEMISTRY

www.rsc.org/softmatter

Cite this: DOI: 10.1039/c0xx00000x

www.rsc.org/xxxxxx

ARTICLE TYPE

Hydrogels assembled from star-shaped polypeptides with dendrimer as core

Yong Shen[a], Shusheng Zhang[a], Yaoming Wan[a], Wenxin Fu[a] and Zhibo Li*[,a,b]

Received (in XXX, XXX) Xth XXXXXXXXX 20XX, Accepted Xth XXXXXXXXX 20XX

DOI: 10.1039/b000000x

Abstract: A second or fourth generation dendrimer with primary amine as peripheral terminal groups was firstly synthesized via Michael addition and thiol-yne addition. A series of star-shaped polypeptide was synthesized by ring opening polymerization (ROP) of γ-(2-(2-methoxyethoxy)ethyl) L-glutamate (L-EG_2Glu) N-carboxyanhydride (NCA) using amine group terminated dendrimer as initiator. Taking advantage of well-defined dendrimer and ROP, the arm number and arm length can be easily controlled. These star-shaped poly(L-EG_2Glu) can spontaneously form hydrogels instead of micelles in water at low concentration. The critical gelation concentration (CGC) and hydrogel strength displayed stronger dependence on arm numbers than the arm length given similar conditions. These properties can be easily modulated by varying poly(L-EG_2Glu) arm length and arm number. The hydrogels showed shear thinning and rapid recovery properties. TEM and AFM characterizations revealed the hydrogel networks were constituted by entangled and branched fibrils.

Introduction

Self-assembled structures based on polypeptides have drawn considerable attention due to their potential applications in biotechnology.[1-3] The most widely investigated amphiphilic diblock copolypeptides can self-assemble to spherical micelles, vesicles, and hydrogel networks, which have been used in drug delivery, gene transfection and tissue scaffold.[4-8] Polypeptides with more complex architecture can lead to hierarchical structures and better mimic cooperative supramolecular interactions existing in proteins. One example is the poly(L-glutamic acid) grafted comb-like polymers developed by Lu and Cheng.[9] The highly branched architecture and directional hydrogen bonding interaction of β-sheet conformation promoted the cooperative self-assembly of long tubular structure.[10] Star-shaped polypeptides, as alternative highly branched polypeptides, can also be used to fabricate high ordered supramolecular structures. Kimura *et. al.* investigated the self-assembly of 8-arm right-handed helical polypeptide with its linear left-handed analogues and found disk structures were formed stoichiometrically.[11] In addition, star-shaped polypeptides were suitable candidates as unimolecular nanoparticles as mimic of dendrimers in drug encapsulation and gene delivery due to the selective enzyme degradation endowed by attached polypeptide.[12-14] Heise and coworkers prepared a series of star-shaped poly(L-glutamic acid) by ROP of amino acid NCAs by utilizing amine groups terminated dendrimer (polypropylene imine) as initiator and investigated enzyme controlled payload release.[14] While most studies focused on the applications of star-shaped polypeptides in drug and gene delivery, few literatures reported their applications as hydrogel scaffold. One example was poly(L-alanine) grafted 4-arm poly(ethylene glycol) (PEG), which formed hydrogel at relatively high concentration around 10 wt%.[15]

Hydrogels assembled from polypeptides are critical biomaterials and have been used in drug delivery, cell therapy and tissue engineering.[16-18] The inherent biodegradability and biocompatibility of polypeptides make them better candidates over the conventional non-degradable polymers in the construction of hydrogels. In addition, the specific secondary structures of polypeptides, such as α-helix and β-sheet, provide additional factors to manipulate the properties of hydrogels besides compositions and architecture. Deming *et. al.* prepared a series of amphiphilic block copolypeptides consisting of polyelectrolytes, *i.e.*, poly(L-lysine) or poly(L-glutamic acid), and hydrophobic segments such as poly(L-leucine) or poly(L-valine). These copolypeptides can spontaneously form hydrogels at low CGC.[19, 20] Furthermore, the hydrogel properties can be manipulated by altering molecular architectures. For example, triblock and pentablock copolypeptides showed higher storage modulus and improved salt stability compared to the diblock copolypeptides with same compositions.[21, 22] Though the hydrogels assembled from polyelectrolyte-b-polypeptide showed tunable properties and unusual high stability to ionic media, the electrostatic attraction between polyelectrolytes and proteins limited their applications *in vivo*. A series of copolymers consisting of PEG and polypeptides were developed to make nonionic hydrogel materials.[23-27] Recently, our group demonstrated the oligo(ethylene glycol) (OEG) functionalized poly(L-glutamate) (poly(L-EG_xGlu)) showed thermo-responsive property in water, and their solution properties strongly depended on their molecular weight and secondary structure.[28, 29] Specially, by utilizing the amphiphilic characteristic of poly(L-EG_2Glu), we

can make nonionic hydrogel by conjugating either hydrophobic alkyl chain or hydrophilic PEG with poly(L-EG_2Glu).[30, 31]

In this contribution, we reported the preparation of star-shaped polypeptides and investigated their self-assembly behaviors in water. It was found the star-shaped poly(L-EG_2Glu) can self-assemble into one dimensional fibrils at low concentration, which then evolved into networks upon increase of concentration. Such unique star-shaped molecular architecture contrast sharply with the previous reported linear poly(L-EG_2Glu) counterparts. Moreover, the hydrogel properties can be easily modulated by varying poly(L-EG_2Glu) arm length and arm number.

Experimental sections

Materials

Tetrahydrofuran (THF), dichloromethane (DCM) and hexane were purified by purging with dry nitrogen, followed by passing through columns of activated alumina. *N,N*-dimethylformamide (DMF) (anhydrous, 99.8%, packaged under Argon in resealable ChemSeal bottles) was purchased from Alfa Aesar. Ethyl acetate (EtOAc) was refluxed with CaH_2 before distillation. Deionized water was obtained from a Millipore Milli-Q purification unit. But-3-yn-1-ol and acryloyl chloride were obtained from Aladdin reagent. L-glutamic acid was obtained from GL Biochem (Shanghai) Ltd. Other reagents were purchased from Aldrich. All commercially obtained reagents were used as received without further purification unless otherwise noted. G2-$[NH_2]_8$, G4-$[NH_2]_{32}$, L-EG_2Glu and the corresponding NCA were synthesized as reported previously.[29, 32]

Instruments

Nuclear magnetic resonance (NMR) spectra were performed on a Bruker AV400 FT-NMR spectrometer (at 400 MHz). The infrared spectroscopy measurements were performed using a Nicolet Avatar 330 FT-IR spectrometer. The samples were prepared by mixing with potassium bromide (KBr) and pressed into disk. Tandem size exclusion chromatography/laser light scattering (SEC/LLS) was performed at 50 °C using an SSI pump connected to Wyatt Optilab DSP and Wyatt DAWN EOS light scattering detectors with 0.02 M LiBr in DMF as eluent at flow rate of 1.0 mL/min. The molecular weight (MW) and polydispersity (PDI) were calculated from the LLS signal by Astra software using the refractive index increment (d*n*/d*c*) of linear poly(L-EG_2Glu) of 0.058 mL/g.[28] The sample concentration used for SEC analysis was about 5 mg/mL. Circular dichroism (CD) spectra were recorded on a Jasco J-815 CD spectropolarimeter. Deionized water was used as reference for baseline correction before measurement. The solution was placed into a quartz cell with a pathlength of 0.1 cm at sample concentration of 0.2 mg/mL. Ellipticity ([θ] in deg·cm^2·dmol^{-1}) was calculated as (millidegrees×mean residue weight)/(pathlength in millimetres× concentration of polypeptide in mg/mL). The α-helix content of the polypeptides was calculated using the following equation: % α-helix=$(-[\theta_{222}]+3000)/39{,}000$.[33] Dynamic light scattering (DLS) was performed on a Malvern Zetasizer Nano ZS instrument. A He–Ne laser (633 nm wavelength) with a fixed detector angle of 173° was used for the measurements. All hydrogel samples were prepared by directly dispersing polypeptide samples in deionized water at room temperature. Transmission electron microscopy (TEM) experiments were performed on a JEM2200FS TEM (200 keV). TEM samples were prepared by spreading sample solution on carbon coated TEM grids and the excess solution or hydrogel was blotted away with a piece of filter paper. Then the samples were negatively stained using 2 wt% aqueous uranyl acetate solution for 30 s. The excess uranyl acetate solution was wicked away using a piece of filter paper. Atomic force microscopy (AFM) was performed in tapping mode (Multimode 8, Bruker, Inc.) with silicon cantilever probes. The scanning rate was 1 Hz. AFM samples were prepared by tapping hydrogels on fresh-cleaved mica disk (diameter 1.0 cm). Scanning electron microscopy (SEM) was performed on a Hitachi S-4300 field-emission scanning electron microscope. The hydrogel samples at 3 wt% concentration were lyophilized before SEM analysis. Then the solid sample was placed on a double-sided sticky carbon tape mounted on aluminum sample holders and then sputter coated with platinum. Rheology measurements were performed on an Anton Paar Modular Compact Rheometer (MCR 502) with 25 mm diameter cone plate geometry and 2° cone angle. All rheology measurements were performed at room temperature through the following procedures. A strain (γ) sweep experiment (γ = 0.001-1) was performed at fixed frequency (ω=1 rad/s) to determine the linear viscoelastic regime. Then a frequency sweep (ω=0.1~100 rad/s) was performed at a constant shear strain (γ = 0.01) to determine the linear storage modulus G'(ω) and linear loss modulus G''(ω). The recovery measurements were performed as following procedures. A large amplitude strain oscillation at γ=1 and ω=6 rad/s for 600 s was used to disrupt the hydrogel structure. Then the storage modulus G'(ω) and loss modulus G''(ω) were determined at the linear viscoelastic regime for 3600 s at γ = 0.01 and ω = 6 rad/s to monitor the recovery of mechanical strength.

Synthesis of star-shaped poly(L-EG_2Glu)

The star-shaped poly(L-EG_2Glu) was designated as Gx-$[NH_2]_m$-$(EG_2Glu)_n$, where x, m, n indicated the dendrimer generation, poly(L-EG_2Glu) arm number, and degree of polymerization (DP) of each arm, respectively. Typically, G2-$[NH_2]_8$-$(EG_2Glu)_n$ was synthesized as following. L-EG_2Glu NCA was dissolved in a mixture of DMF/THF (V:V = 1:1) under nitrogen. A prescribed quantity of G2-$[NH_2]_8$ was dissolved in minimum anhydrous THF and immediately injected into the above solution. The polymerization was conducted under nitrogen at room temperature and monitored by FT-IR. Once the NCA was completely consumed, the reaction mixture was precipitated into ethyl ether 3 times. Products were collected by centrifugation and dried under reduced pressure to give white solid. The polypeptide chain length of each arm was tuned by varying the molar ratio of L-EG_2Glu NCA to G2-$[NH_2]_8$. G4-$[NH_2]_{32}$-$(EG_2Glu)_n$ was prepared in a similar method except using G4-$[NH_2]_{32}$ as initiator. ^{1}H NMR ($CDCl_3$/CF_3COOD (V:V = 1:1), 400MHz): δ (ppm): 4.64 (m, 1H), 4.32 (m, 2H), 3.87-3.80 (m, 6H), 3.53 (s, 3H), 2.56 (m, 2H), 2.18 (m, 1H), 2.02 (m, 1H). ^{13}C NMR ($CDCl_3$/CF_3COOD (V:V = 1:1), 100MHz): δ (ppm): 176.1, 173.7, 71.4, 69.9, 69.2, 64.6, 58.5, 53.9, 30.4, 27.5. All samples gave similar and consistent NMR spectra.

Cite this: DOI: 10.1039/c0xx00000x

www.rsc.org/xxxxxx

ARTICLE TYPE

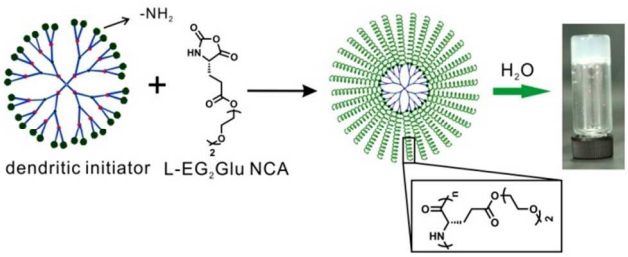

Scheme 1. Illustration of the synthesis of star-shaped poly(L-EG_2Glu).

Results and discussion

Generally, polypeptides can be prepared via ROP of amino acid NCAs initiated by primary amine, strong bases, transition metal catalysts and recently developed organosilicon amines.[34-36] Among them, primary amine is the most frequently used initiator for the synthesis of linear polypeptides due to its feasibility and availability. In this study, we employed primary amine group terminated dendrimer as initiator to construct star-shaped poly(L-EG_2Glu). The synthetic protocol of dendrimer and L-EG_2Glu NCA were reported elsewhere.[29, 32]

Two series of star-shaped samples were prepared based on G2-$[NH_2]_8$ and G4-$[NH_2]_{32}$ two dendrimers, which has 8 or 32 peripheral primary amine groups, respectively (**Scheme 1**). In addition to the arm number, star-shaped poly(L-EG_2Glu) with different arm length were prepared by varying the feed ratio of L-EG_2Glu NCA monomer to dendrimer initiator. The MW and PDI were characterized using SEC equipped with multi-angle light scattering detectors. The *dn/dc* = 0.058 mL/g obtained from linear poly(L-EG_2Glu) was used to determine the MW of star-shaped polypeptides. **Table 1** summarizes the corresponding molecular parameters of obtained samples. For the first set of samples, G2-$[NH_2]_8$ was used as initiator, and the feed ratio of L-EG_2Glu NCA to initiator was varied from 15 to 50 (entry 1-4, **Table 1**). As shown in **Figure 1**, the MWs increase linearly with the feed ratio of NCA to amine groups, and the obtained MW agreed well with

Table 1. The molecular parameters and critical gelation concentration (CGC) of different samples used in this study.

Entry	Sample	NCA/$[NH_2]$ feed ratio	Theoretical M_n[a] (kDa)	Mn[b] (kDa)	PDI[b]	CGC (wt%)[c]
1	G2-$[NH_2]_8$-$(EG_2Glu)_{15}$	15	28.9	34.6	1.05	3
2	G2-$[NH_2]_8$-$(EG_2Glu)_{20}$	20	38.2	36.3	1.17	3
3	G2-$[NH_2]_8$-$(EG_2Glu)_{30}$	30	56.7	58.8	1.13	2
4	G2-$[NH_2]_8$-$(EG_2Glu)_{50}$	50	93.7	86.8	1.32	3
5	G4-$[NH_2]_{32}$-$(EG_2Glu)_{15}$	15	117	80.6	1.57	2
6	G4-$[NH_2]_{32}$-$(EG_2Glu)_{30}$	30	228	131	1.91	1

[a] Theoretical M_n was calculated assuming all amine groups initiated ROP and the quantitative conversion of NCA monomers; [b] determined by SEC with light scattering detectors; [c] determined by the inverted tube method. The samples were considered to be a gel if no flow happened within 30 s after inverting the tube.

expected values, which suggested a well-controlled ROP of L-EG_2Glu NCA. In addition, all samples gave relative narrow PDI and symmetrical unimodal SEC trace. These results demonstrated the applicability of the method to prepare star-shaped poly(L-EG_2Glu) with controllable arm length by utilizing amine terminated dendrimer as initiator. In contrast, the synthesis became less controllable over arm length with increase of arm numbers. There were two possible reasons for such deviations compared to previous example. One was probably due to the highly branched structure of G4-$[NH_2]_{32}$-$(EG_2Glu)_n$ than G2-$[NH_2]_8$-$(EG_2Glu)_n$. The former bears more initiation sites and relative larger PDI than the latter due to challenge in dendrimer synthesis. The other reason might arise from the use of non-ideal *dn/dc* value in MW calculation.[14] Moreover, it is worth noting that G4-$[NH_2]_{32}$-$(EG_2Glu)_n$ had a relative broader PDI compared to G2-$[NH_2]_8$-$(EG_2Glu)_n$ counterparts. One possible reason is the relative broad PDI of the dendritic initiator, *i.e.*, G4-$[NH_2]_{32}$. The tertiary amines existing in the dendrimer core may also initiate the polymerization through the "activated monomer mechanism" and resulted in the formation of linear poly(L-EG_2Glu), which also led to a broader distribution of final product. The broader PDI and existing of linear poly(L-EG_2Glu) may be also responsible for the under-estimated MWs for 32-arm G4-$[NH_2]_{32}$-$(EG_2Glu)_n$. ^1H and ^{13}C NMR spectroscopy was used to further characterize the star-shaped poly(L-EG_2Glu) samples. **Figure S1** presents the ^1H and ^{13}C NMR spectra of G2-$[NH_2]_8$-$(EG_2Glu)_{15}$. Due to the relative small dendrimer core compared to the polypeptide shell, it was difficult to distinguish the proton signals of dendrimer core from these NMR spectra. Though it

Cite this: DOI: 10.1039/c0xx00000x

www.rsc.org/xxxxxx

ARTICLE TYPE

was not easy to determine the MW from the NMR spectra default of internal reference, the unambiguous assignment of each resonance peak verified the successful grafting of poly(L-EG_2Glu) from G2-$[NH_2]_8$. Other samples gave similar and consistent NMR spectra with G2-$[NH_2]_8$-$(EG_2Glu)_{15}$ (data not show).

The star-shaped poly(L-EG_2Glu) with a hydrophobic core and a relative hydrophilic corona is supposed to form unimolecular micelles when dispersed in water. Considering the amphiphilic characteristic and conformation associated hydrogen bonding interaction of poly(L-EG_2Glu) arms, these star-shaped poly(L-EG_2Glu) may self-assemble to hierarchical structures. We firstly dispersed these star-shaped polypeptides in deionized water, but did not observe ordered structures from TEM characterization. Interestingly, all samples spontaneously self-assembled to hydrogels at low concentration. The gelation time varied from tens of minutes to several hours, and mechanical vortex can facilitate gelation. The CGC was determined using inverted tube method. As shown in **Table 1**, the CGC displayed apparently stronger dependence on arm number than MW of each arm. For example, G2-$[NH_2]_8$-$(EG_2Glu)_{15}$ had CGC of 3 wt% while sample G4-$[NH_2]_{32}$-$(EG_2Glu)_{15}$ had CGC of 2wt%. Also, G4-$[NH_2]_{32}$-$(EG_2Glu)_{30}$ formed hydrogel at 1 wt%, which was half of G2-$[NH_2]_8$-$(EG_2Glu)_{30}$. Note that these hydrogel was not stable in ionic media.

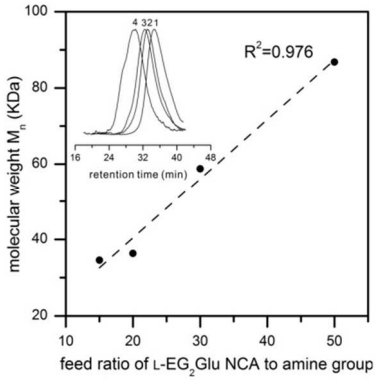

Figure 1. The MW dependence of star-shaped polypeptide on the feed ratio of L-EG_2Glu NCA to amine group for G2-$[NH_2]_8$-$(EG_2Glu)_n$ series (the insert figure gives the SEC traces of entry 1 to 4).

Rheology was then applied to characterize the hydrogel strength at different conditions. A strain sweep experiment was firstly conducted for all samples to determine the linear viscoelastic regime. The frequency sweep measurements conducted in linear regime then gave the corresponding storage modulus G' and loss modulus G''. **Figure S2, S3, S4** gave the results for G2-$[NH_2]_8$-$(EG_2Glu)_{30}$, G4-$[NH_2]_{32}$-$(EG_2Glu)_{15}$ and G4-$[NH_2]_{32}$-$(EG_2Glu)_{30}$, respectively, at different concentrations. All samples were determined to be solid gel over the experimental frequency range and concentrations since the G' was one order of magnitude larger than G''. Both storage modulus G' and loss modulus G'' increased as concentration increased. For example, the storage modulus of G4-$[NH_2]_{32}$-$(EG_2Glu)_{30}$ increased from 47 to 3355 Pa as concentration increased from 2 wt% to 4 wt%.

We further performed the rheology measurements for G2-$[NH_2]_8$-$(EG_2Glu)_{15}$, G2-$[NH_2]_8$-$(EG_2Glu)_{20}$ and G2-$[NH_2]_8$-$(EG_2Glu)_{50}$ aqueous solution at 3 wt% concentration to explore the effects of arm length and number on hydrogel strength. As indicated in **Figure 2a**, the storage modulus increased from 24 Pa to 350 Pa as the DP of poly(L-EG_2Glu) arm increased from 15 to 50 for G2-$[NH_2]_8$-$(EG_2Glu)_n$ samples at 3 wt% concentration (at frequency ω = 6 rad/s and strain γ = 0.01). In addition to the arm length, the arm number also played an important role on the hydrogel strength. When fixed the arm length at 30, G4-$[NH_2]_{32}$-$(EG_2Glu)_{30}$ (G'= 1370 Pa at ω = 6 rad/s, γ = 0.01) showed a much higher modulus than that of G2-$[NH_2]_8$-$(EG_2Glu)_{30}$ (G'= 240 Pa at ω = 6 rad/s, γ = 0.01).We assumed that increasing both poly(L-EG_2Glu) arm length and arm number strengthened the hydrogen bonding interactions among star-shaped poly(L-EG_2Glu) and increased the physical crosslinking density of hydrogel networks, which induced the increase in hydrogel strength. It is worth pointing out that the hydrogel strength can be modulated from 24 Pa to 3350 Pa by simply adjusting the sample compositions and concentrations to meet specific application requirements. Such a broad adjustable range was not available in the previous reported linear poly(L-EG_2Glu) systems.[30, 31]

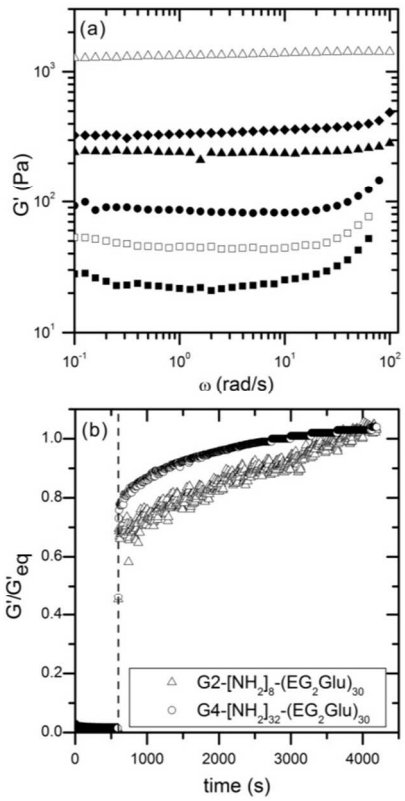

Figure 2. (a) Storage modulus G' as a function of angular frequency for samples G2-$[NH_2]_8$-$(EG_2Glu)_{15}$ (■), G2-$[NH_2]_8$-$(EG_2Glu)_{20}$ (●), G2-$[NH_2]_8$-$(EG_2Glu)_{30}$ (▲), G2-$[NH_2]_8$-$(EG_2Glu)_{50}$ (◆), G4-$[NH_2]_{32}$-$(EG_2Glu)_{15}$ (□), and G4-$[NH_2]_{32}$-$(EG_2Glu)_{30}$ (△) aqueous solutions (γ = 0.01) at 3.0 wt % concentrations; (b) G'/G'_{eq} as a function of time for hydrogels G2-$[NH_2]_8$-$(EG_2Glu)_{30}$ (△), G4-$[NH_2]_{32}$-$(EG_2Glu)_{30}$ (○) , which were sheared at ω = 6 rad/s, γ = 1 for 600 s before switching to small strain. The hydrogel strength was monitored through small amplitude oscillations at ω = 6 rad/s, γ = 0.01.

Akin to the alkyl-poly(L-EG_2Glu) hydrogel, the star-shaped poly(L-EG_2Glu) hydrogel also displayed shear thinning and rapid recovery properties. **Figure 2b** gave the recovery measurements for G2-$[NH_2]_8$-$(EG_2Glu)_{30}$ and G4-$[NH_2]_{32}$-$(EG_2Glu)_{30}$ at 3 wt% concentration. Upon imposing a large amplitude shear strain, ca. γ = 1, the storage modulus G' for both G2-$[NH_2]_8$-$(EG_2Glu)_{30}$ and G4-$[NH_2]_{32}$-$(EG_2Glu)_{30}$ samples dropped by two orders of magnitude and underwent a gel-sol transition. As shown in **Figure 2b**, the G2-$[NH_2]_8$-$(EG_2Glu)_{30}$ and G4-$[NH_2]_{32}$-$(EG_2Glu)_{30}$ hydrogel recovered to a gel state within 10 s after switching to a small amplitude shear strain (γ=0.01). Particularly, G2-$[NH_2]_8$-$(EG_2Glu)_{30}$ regained 69% original strength and G4-$[NH_2]_{32}$-$(EG_2Glu)_{30}$ hydrogel regained 76% original strength within 10 seconds, after which both samples continued to recover their strength progressively and reached 100% recovery of original strength within 1 hour. The shear thinning and rapid recovery properties made these star-shaped poly(L-EG_2Glu) suitable candidates as potential injectable hydrogel materials in biomedical applications. To verify this point, we performed the injection experiment using 3 wt % G2-$[NH_2]_8$-$(EG_2Glu)_{30}$ hydrogel as example. (Video in the supporting information)

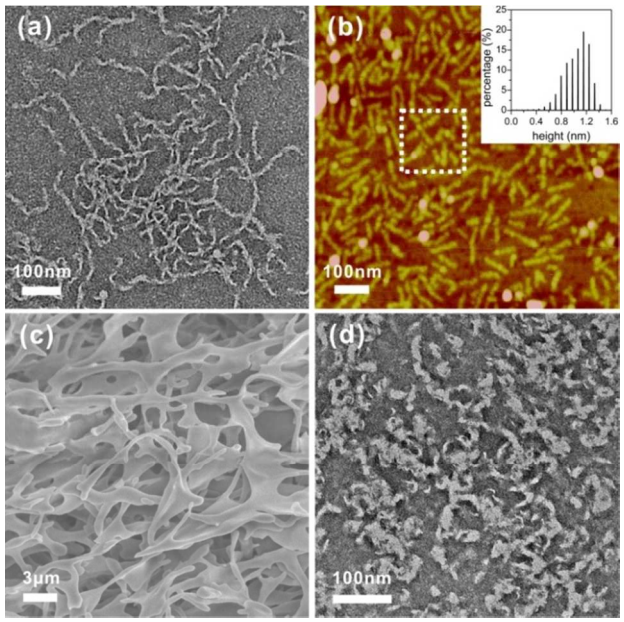

Figure 3. (a) TEM image, (b) AFM height image, and (c) SEM image of G2-$[NH_2]_8$-$(EG_2Glu)_{30}$ hydrogel sample at 3 wt% concentration, (d) TEM image of G4-$[NH_2]_{32}$-$(EG_2Glu)_{30}$ hydrogel sample at same concentration. The inset in AFM height image indicates the corresponding height histogram of the white frame.

TEM and AFM were used to characterize the nanostructures of a typical hydrogel sample. As shown in **Figure 3a**, G2-$[NH_2]_8$-$(EG_2Glu)_{30}$ formed fibril assemblies. The average width calculated from five different TEM images was 16.3±1.9 nm, and the fibril length ranged from 100 nm to several micrometers. The AMF height image further verified G2-$[NH_2]_8$-$(EG_2Glu)_{30}$ self-assembled to one dimensional fibrils, whose average width and height calculated from AFM height images was 22.2±1.2 nm and 1.1±0.4 nm, respectively. Considering the highly branched molecular architecture of G2-$[NH_2]_8$-$(EG_2Glu)_{30}$, the one dimensional fibril assemblies were not stable and should evolve to higher ordered structures. **Figure 3c** gave the SEM image of the lyophilized G2-$[NH_2]_8$-$(EG_2Glu)_{30}$ hydrogel sample, which indicated the one dimensional fibrils tended to further entangle to form complex sheet-like assemblies. In contrast, G4-$[NH_2]_{32}$-$(EG_2Glu)_{30}$, which has comparable chain length but more arms relative to G2-$[NH_2]_8$-$(EG_2Glu)_{30}$, cannot form ordered assemblies at the same concentration (**Figure 3d**).

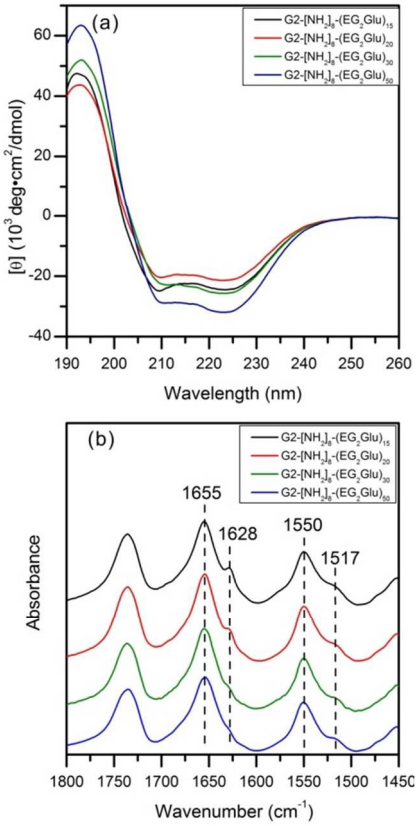

Figure 4. (a) CD spectra and (b) FT-IR spectra of G2-$[NH_2]_8$-$(EG_2Glu)_n$ samples.

It is well known that the secondary structures play an important role on the polypeptide hydrogel properties. We applied circular dichroism (CD) and FT-IR spectroscopy to explore the effects of poly(L-EG_2Glu) arm length and arm number on the conformation of star-shaped polypeptide. **Figure 4a** compares the CD spectra of G2-$[NH_2]_8$-$(EG_2Glu)_n$ with n varied between 15 and 50. All samples showed a positive peak around 193 nm and two negative peaks at 209 nm and 222 nm, indicative of α-helical conformation. The α-helix content increased with increasing poly(L-EG_2Glu) arm length, which was consistent with the previous reported linear poly(L-EG_2Glu) homopolypeptide.[28] Specifically, the α-helix content increased from 70% for G2-$[NH_2]_8$-$(EG_2Glu)_{15}$ to 89% for G2-$[NH_2]_8$-$(EG_2Glu)_{50}$. In addition to arm length, arm number also affected the secondary structure of star-shaped poly(L-EG_2Glu). G4-$[NH_2]_{32}$-$(EG_2Glu)_{15}$ and G4-$[NH_2]_{32}$-$(EG_2Glu)_{30}$, showed similar CD spectra but overall lower intensity compared to their 8-arm counterparts, suggesting the α-helix content decreased with increasing arm numbers (**Figure S5a**). We speculated two reasons were responsible for the lower α-helix content. One is the existence of shorter chain relative to the theoretical value as indicated by broad PDI. Compared to G2-$[NH_2]_8$-$(EG_2Glu)_n$, G4-$[NH_2]_{32}$-$(EG_2Glu)_n$ with same poly(L-EG_2Glu) arm length formed hydrogels at much lower concentration. This result suggested G4-$[NH_2]_{32}$-$(EG_2Glu)_n$ would self-assemble into more ordered assemblies. The formation of assemblies at low concentration may also decrease the overall intensity in the CD spectra. This assumption was supported by the DLS experiment, which verified that the assembly formed by G4-$[NH_2]_{32}$-$(EG_2Glu)_n$ was tens of nanometers even at concentration as low as 0.1mg/mL.

FT-IR spectra were further used to investigate the polypeptide conformation of star-shaped poly(L-EG_2Glu) in solid state. All samples revealed strong amide I band absorption and amide II band absorption, located at 1655 and 1550 cm^{-1}, respectively, which suggested existence of predominant α-helical conformation (**Figure 4b**). For samples G2-$[NH_2]_8$-$(EG_2Glu)_{15}$ and G2-$[NH_2]_8$-$(EG_2Glu)_{20}$, which had shorter arm length, the obvious shoulder peak at 1628 cm^{-1} (amide Ⅰ band) and 1517 cm^{-1} (amide Ⅱ band) suggested the coexistence of β-sheet conformation. Given comparable arm length and increased arm number, G4-$[NH_2]_{32}$-$(EG_2Glu)_n$ (n = 15, 30) had similar FT-IR spectra with G2-$[NH_2]_8$-$(EG_2Glu)_n$ (n = 15, 30) (**Figure S5b**). Through deconvolution of amide I band in FT-IR spectra, semi-quantitative calculations for secondary structure contents were summarized in **Table S1**. For G2-$[NH_2]_8$-$(EG_2Glu)_n$ series, the α-helix content increased with increased poly(L-EG_2Glu) arm length while the β-sheet content showed opposite tendency. Given comparable arm length, G4-$[NH_2]_{32}$-$(EG_2Glu)_n$ showed slightly lower α-helix content and higher β-sheet content than their 8-arm counterparts. These results agreed well with the CD data discussed above, suggesting the secondary structures were mainly dominated by poly(L-EG_2Glu) arm length.

Generally, two different self-assembled structures were proposed to explain the formation of three dimensional hydrogel networks, *i.e.*, packing of spherical micelles and elongated fibrils. The star-shaped poly(L-EG_2Glu) with a hydrophobic core and a relatively hydrophilic corona seemed to prefer forming unimolecular micelles. However, micellar systems form elastic hydrogels only when the micelles pack into ordered arrays, which require a relatively high concentration of 5-10 wt%. Apparently, such a model cannot explain the fibrils observed by TEM and the low CGC of the star-shaped poly(L-EG_2Glu). **Figure S7a-c** gave the TEM images of G2-$[NH_2]_8$-$(EG_2Glu)_{30}$ aqueous solutions at concentration of 0.03 wt%, 0.3 wt% and 3 wt%, respectively. Apparently, G2-$[NH_2]_8$-$(EG_2Glu)_{30}$ still assembled into fibrils instead of spherical micelles even at concentration as low as 0.03 wt%. Given fibrillar nanostructure, it was expected that hydrogel networks would form with increase of concentration. This self-assembly behaviour of star-shaped poly(L-EG_2Glu) could be attributed to the amphiphilic characteristic and conformation associated hydrogen bonding interactions of poly(L-EG_2Glu) arms. In contrast to the conventional polymers, the hydrogen bonding interactions among poly(L-EG_2Glu) arms destabilized the unimolecular micelles and promoted self-assembly. On the other hand, it is well known that linear peptide amphiphiles can self-assemble into elongated fibrils or nanoribbons driven by β-sheet conformation. The previous reported alkyl-poly(L-EG_2Glu) and PEG-b-poly(L-EG_2Glu) systems showed highly ordered nanoribbon structures due to the directional hydrogen bonding among poly(L-EG_2Glu) segments. Moreover, the hydrogel formed by alkyl-poly(L-EG_2Glu) and PEG-b-poly(L-EG_2Glu) showed increased strength with increased β-sheet conformation content.[30, 31] In contrast, the star-shaped poly(L-EG_2Glu) mainly adopted α-helical conformation. Accordingly, we proposed that the fibrils were formed predominately by the oriented parallel or anti-parallel packing of rigid α-helix while the hydrophilic OEG side chain conferred the solubility of fibrils. While the OEG side

chains conferred the solubility of star-shaped poly(L-EG_2Glu) albeit their solution contribution not as good as we expected. However, such "suitable" solubility assured the hydrophilic/hydrophobic balance and was necessary for the hydrogel formation. In contrast, both poly(L-EG_1Glu) and poly(L-EG_3Glu) cannot form hydrogels. The poly(L-EG_1Glu) with shorter OEG side chain cannot dissolve in water while poly(L-EG_3Glu) with longer OEG side chain can only form aqueous solution.This model is similar with the poly(L-lysine)-b-poly(L-leucine) system reported by Deming.[19-21] Unfortunately, it is difficult to figure out an unambiguous model on the molecular level to explain the self-assembly of the star-shaped poly(L-EG_2Glu) according to the available data. Nevertheless, we can speculate that increasing the poly(L-EG_2Glu) arm length can increase the α-helix content and promote the ordered packing of α-helix. The increased interactions between α-helix in turn strengthen the hydrogel and reduce the CGC. On the other hand, increasing the arm number of the star-shaped poly(L-EG_2Glu) will promote the branching and entanglement of the fibrils, which is favored in the formation of interconnected three dimensional networks. As a consequence, G4-$[NH_2]_{32}$-$(EG_2Glu)_n$ showed higher storage modulus and lower CGC than their 8-arm counterparts. It also accounts for the irregular aggregates formed by G4-$[NH_2]_{32}$-$(EG_2Glu)_{30}$ instead of elongated fibrils.

Compared to the previous reported linear block copolypeptides, *i.e.,* alkyl-poly(L-EG_2Glu) and PEG-b-poly(L-EG_2Glu), the star-shaped poly(L-EG_2Glu) showed distinct intriguing properties. The alkyl-poly(L-EG_2Glu) can form hydrogel only when the degree of polymerization of poly(L-EG_2Glu) is around 10. Even if the subtle variation in the chain length will disrupt the perfect hydrophilic/hydrophobic balance and result in the failure of hydrogel formation. For example, dodecyl-poly(L-$EG_2Glu)_{20}$ with a slightly longer chain was almost insoluble in water and can not form hydrogel even at 10 wt% concentration. The PEG_{44}-b-poly(L-$EG_2Glu)_x$ system allowed a relative broader variation in poly(L-EG_2Glu) chain length from x = 16 to 25. PEG_{44}-b-poly(L-$EG_2Glu)_x$ diblock copolymers with x larger than 40 formed cylindrical micelles and showed thermal annealing induced self-assembly behavior. Besides, PEG-b-poly(L-EG_2Glu) can only form weak hydrogels with storage modulus smaller than 100 Pa. In contrast, the star-shaped poly(L-$EG_2Glu)_x$ can form hydrogels at a quite broad range of chain length (x = 15~50). Moreover, the hydrogel strength can be modulated from 24 Pa to 3350 Pa to meet specific application requirements by simply adjusting the sample compositions and concentrations as discussed above.

Conclusions

Using amine group terminated dendrimer as initiators, we prepared a series of star-shaped polypeptide through ROP of L-EG_2Glu NCA. These star-shaped poly(L-EG_2Glu) can spontaneously self-assemble to hydrogel in water. Given similar poly(L-EG_2Glu) arm length, samples with 32 arms had lower CGCs than samples with 8 arms. The hydrogel strength was strongly dependent on the poly(L-EG_2Glu) arm length and arm number. In contrast to linear alkyl-b-poly(L-EG_2Glu) hydrogel system driven by β-sheet conformation, the ordered packing of rigid α-helix accounted for the formation of fibrils, which further entangled and branched to form three dimensional hydrogel networks in such star shaped polypeptide system. The hydrogel formed by star-shaped poly(L-EG_2Glu) showed shear thinning and rapid recovery properties and can be used as injectable hydrogel for controlled peptide drug release system.

Acknowledgements

This work was financially supported by the NSFC Funding for Distinguished Young Scholar (51225306) and NSFC (21434008).

Notes and references

[a] *Laboratory of Polymer Physics and Chemistry, Institute of Chemistry, Chinese Academy of Sciences, Beijing 100190, China; E-mail: zbli@iccas.ac.cn*

[b] *School of Polymer Science and Engineering, Qingdao University of Science and Technology, Qingdao 266042, China;*

† Electronic Supplementary Information (ESI) available: Additional NMR spectra, rheology data, TEM images, CD and FTIR spectra, video of the injection experiment for 3 wt% G2-$[NH_2]_8$-$(EG_2Glu)_{30}$ hydrogel. See DOI: 10.1039/b000000x/

1. Y. Shen, X. Fu, W. Fu and Z. Li, *Chem. Soc. Rev.*, 2015, **44**, 612-622.
2. C. He, X. Zhuang, Z. Tang, H. Tian and X. Chen, *Adv. Healthcare Mater.*, 2012, **1**, 48-78.
3. C. Deng, J. Wu, R. Cheng, F. Meng, H.-A. Klok and Z. Zhong, *Prog. Polym. Sci.*, 2014, **39**, 330-364.
4. H. Peng, Y. Xiao, X. Mao, L. Chen, R. Crawford and A. K. Whittaker, *Biomacromolecules*, 2009, **10**, 95-104.
5. J. Huang, C. Bonduelle, J. Thévenot, S. Lecommandoux and A. Heise, *J. Am. Chem. Soc.*, 2012, **134**, 119-122.
6. B. Song, J. Song, S. Zhang, M. A. Anderson, Y. Ao, C.-Y. Yang, T. J. Deming and M. V. Sofroniew, *Biomaterials*, 2012, **33**, 9105-9116.
7. S. Takae, K. Miyata, M. Oba, T. Ishii, N. Nishiyama, K. Itaka, Y. Yamasaki, H. Koyama and K. Kataoka, *J. Am. Chem. Soc.*, 2008, **130**, 6001-6009.
8. N. P. Gabrielson, H. Lu, L. Yin, D. Li, F. Wang and J. Cheng, *Angew. Chem. Int. Ed.*, 2012, **51**, 1143-1147.
9. H. Lu, J. Wang, Y. Lin and J. Cheng, *J. Am. Chem. Soc.*, 2009, **131**, 13582-13583.
10. J. Wang, H. Lu, R. Kamat, S. V. Pingali, V. S. Urban, J. Cheng and Y. Lin, *J. Am. Chem. Soc.*, 2011, **133**, 12906-12909.
11. H. Matsui, M. Ueda, A. Makino and S. Kimura, *Chem. Commun.*, 2012, **48**, 6181-6183.
12. H. Huang, J. Li, L. Liao, J. Li, L. Wu, C. Dong, P. Lai and D. Liu, *Eur. Polym. J.*, 2012, **48**, 696-704.
13. H. M. Wu, S. R. Pan, M. W. Chen, Y. Wu, C. Wang, Y. T. Wen, X. Zeng and C. B. Wu, *Biomaterials*, 2011, **32**, 1619-1634.
14. M. Byrne, P. D. Thornton, S. A. Cryan and A. Heise, *Polym. Chem.*, 2012, **3**, 2825-2831.
15. P. D. Thornton, S. M. R. Billah and N. R. Cameron, *Macromol. Rapid Commun.*, 2013, **34**, 257-262.
16. U. P. Shinde, M. K. Joo, H. J. Moon and B. Jeong, *J. Mater. Chem.*, 2012, **22**, 6072-6079.
17. E. J. Yun, B. Yon, M. K. Joo and B. Jeong, *Biomacromolecules*, 2012, **13**, 1106-1111.
18. Y. Jeong, M. K. Joo, K. H. Bahk, Y. Y. Choi, H.-T. Kim, W.-K. Kim, H. Jeong Lee, Y. S. Sohn and B. Jeong, *J. Control. Release*, 2009, **137**, 25-30.
19. A. P. Nowak, V. Breedveld, L. Pakstis, B. Ozbas, D. J. Pine, D. Pochan and T. J. Deming, *Nature*, 2002, **417**, 424-428.
20. A. P. Nowak, V. Breedveld, D. J. Pine and T. J. Deming, *J. Am. Chem. Soc.*, 2003, **125**, 15666-15670.
21. V. Breedveld, A. P. Nowak, J. Sato, T. J. Deming and D. J. Pine, *Macromolecules*, 2004, **37**, 3943-3953.

22. Z. Li and T. J. Deming, *Soft Matter*, 2010, **6**, 2546-2551.
23. Y. Cheng, C. He, C. Xiao, J. Ding, X. Zhuang, Y. Huang and X. Chen, *Biomacromolecules*, 2012, **13**, 2053-2059.
24. Y. Y. Choi, M. K. Joo, Y. S. Sohn and B. Jeong, *Soft Matter*, 2008, **4**, 2383-2387.
25. H. J. Oh, M. K. Joo, Y. S. Sohn and B. Jeong, *Macromolecules*, 2008, **41**, 8204-8209.
26. Y. Y. Choi, J. H. Jang, M. H. Park, B. G. Choi, B. Chi and B. Jeong, *J. Mater. Chem.*, 2010, **20**, 3416-3421.
27. J. Huang, C. L. Hastings, G. P. Duffy, H. M. Kelly, J. Raeburn, D. J. Adams and A. Heise, *Biomacromolecules*, 2013, **14**, 200-206.
28. S. Zhang, C. Chen and Z. Li, *Chin. J. Polym. Sci.*, 2013, **31**, 201-210.
29. C. Chen, Z. Wang and Z. Li, *Biomacromolecules*, 2011, **12**, 2859-2863.
30. S. Zhang, W. Fu and Z. Li, *Polym. Chem.*, 2014, **5**, 3346-3351.
31. C. Chen, D. Wu, W. Fu and Z. Li, *Biomacromolecules*, 2013, **14**, 2494-2498.
32. Y. Shen, Y. Ma and Z. Li, *J. Polym. Sci., Part A: Polym. Chem.*, 2013, **51**, 708-715.
33. J. A. Morrow, M. L. Segall, S. Lund-Katz, M. C. Phillips, M. Knapp, B. Rupp and K. H. Weisgraber, *Biochemistry*, 2000, **39**, 11657-11666.
34. H. Lu, J. Wang, Z. Song, L. Yin, Y. Zhang, H. Tang, C. Tu, Y. Lin and J. Cheng, *Chem. Commun.*, 2014, **50**, 139-155.
35. N. Hadjichristidis, H. Iatrou, M. Pitsikalis and G. Sakellariou, *Chem. Rev.*, 2009, **109**, 5528-5578.
36. J. Cheng and T. J. Deming, *Top. Curr. Chem.*, 2012, **310**, 1-26.

For Table of Contents use only

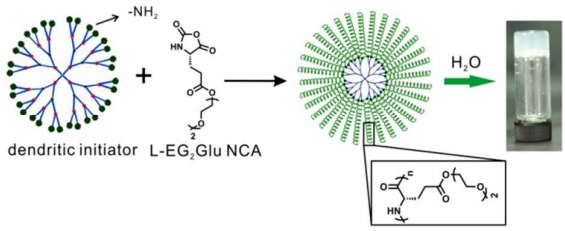

In this work, we reported the facile preparation of novel star-shaped polypeptides, which self-assemble into hydrogels at low critical gelation concentration.